Modeling the ratios of SKKS and SKS amplitudes with ultra-low velocity zones at the core-mantle boundary

Yang Zhang,[1] Jeroen Ritsema,[1] and Michael S. Thorne[2]

Received 16 July 2009; revised 18 August 2009; accepted 3 September 2009; published 3 October 2009.

[1] Between 105–115° degrees, the SKS waveform is complicated by the formation of SP_dKS, a wave that has segments of P diffraction along the core mantle boundary. While previous studies have primarily focused on the move-out of SP_dKS from SKS, we analyze the concomitant reduction of the SKS amplitude. Long-period SKKS/SKS amplitude ratios present a coherent global pattern. SKKS/SKS is relatively large in North and South American recordings of deep Tonga-Fiji earthquakes but PREM-like in European recordings of earthquakes in South America and North American recordings of earthquakes in Indonesia. Modeling of SKKS/SKS indicate that Ultra-Low Velocity Zones (ULVZs), layers at the base of the mantle with a thickness of about 10–20 km and a shear velocity reduction between 20–30%, are required to explain high SKKS/SKS ratios and the early move-out of SP_dKS. **Citation:** Zhang, Y., J. Ritsema, and M. S. Thorne (2009), Modeling the ratios of SKKS and SKS amplitudes with ultra-low velocity zones at the core-mantle boundary, *Geophys. Res. Lett.*, *36*, L19303, doi:10.1029/2009GL040030.

1. Introduction

[2] Joint seismological and mineral physics studies have suggested that silicate melts are present at the base of the mantle [e.g., *Williams and Garnero*, 1996; *Hernlund and Tackley*, 2007]. Seismically, these melt structures can be modeled as 10–40 km thick layers with extreme (10–40%) reductions in shear velocity [e.g., *Thorne and Garnero*, 2004]. These Ultra-Low Velocity Zones (ULVZs) in general have variable shapes, widths, and distributions across the core-mantle boundary (CMB). The best studied ULVZ is located at the margins of a low seismic velocity anomaly beneath the Pacific [e.g., *Garnero et al.*, 1998; *Simmons and Grand*, 2002; *Ni and Helmberger*, 2003].

[3] So far, ULVZs have been modeled primarily using SP_dKS traveltimes [e.g., *Garnero and Helmberger*, 1996; *Rondenay and Fischer*, 2003] and PcP and ScP reflections [e.g., *Rost and Revenaugh*, 2001, 2003; *Rost and Garnero*, 2006; *Idehara et al.*, 2007; *Hutko et al.*, 2009]. Here, we demonstrate that the frequency-dependent amplitude ratio of the seismic phases SKKS and SKS can provide complementary constraints.

[1]Department of Geological Sciences, University of Michigan, Ann Arbor, Michigan, USA.
[2]Department of Geology and Geophysics, University of Utah, Salt Lake City, Utah, USA.

0094-8276/09/2009GL040030

2. SKKS/SKS Amplitude Ratio

[4] Since SKS and SKKS waves propagate along similar paths in the upper mantle, anomalous traveltime [e.g., *Souriau and Poupinet*, 1991] and amplitude [e.g., *Silver and Bina*, 1993] differences are excellent indicators of deep mantle heterogeneity (Figure 1). SKS bifurcates near a distance of about 104° (depending on source depth) for PREM [*Dziewonski and Anderson*, 1981]. At this distance, SP_dKS, a wave that includes segments of P diffraction along the CMB develops [*Choy*, 1977] and SKS decreases in amplitude. However, SP_dKS forms earlier when ULVZs are present. Consequently, the difference time between SP_dKS and SKS and the amplitude ratios of SKKS and SKS are larger than expected for PREM.

[5] We define the SKKS/SKS amplitude ratio as

$$R = \log_{10}\left(\frac{A_{\mathrm{SKKS}}}{A_{\mathrm{SKS}}}\right) - \log_{10}\left(\frac{A_{\mathrm{SKKS}}}{A_{\mathrm{SKS}}}\right)_{\mathrm{REF}} \quad (1)$$

where the second term is determined for the PREM velocity structure and Global CMT event parameters. Figure 2 shows two examples of SKS and SKKS recordings and PREM synthetics of the October 16, 2007 (Depth = 512 km, M_w = 6.6) Fiji Islands earthquake at stations CCM and FVM in Missouri. These recordings are representative of the signal quality of SKS and SKKS and they illustrate that variability in R is evident even for nearby stations.

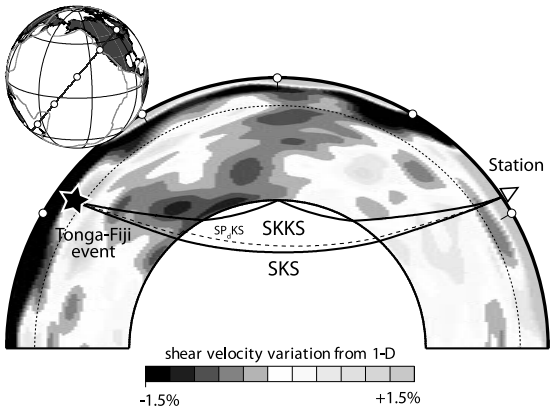

Figure 1. Geometrical ray paths of SKS, SKKS (solid lines) and SP_dKS (dashed line) propagating from a deep earthquake in the Tonga-Fiji region (dark circle) to a North American station (light circles) at an epicentral distance of 110°. The background shows the shear velocity variation in the mantle according to *Ritsema et al.* [1999]. The shear velocity in regions shaded dark (light) grey is lower (higher) than in PREM.

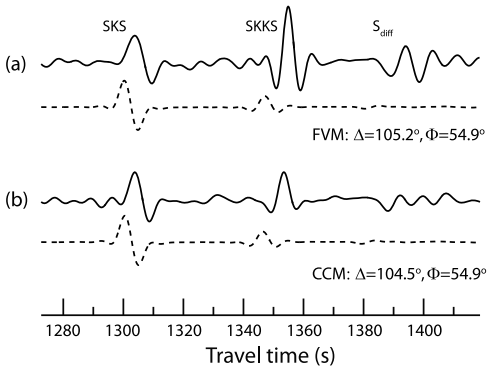

Figure 2. Radial component observed (solid) and synthetic (dashed) seismograms at stations (a) FVM (French Village, Missouri) and (b) CCM (Cathedral Cave, Missouri) from Global-CMT event C200710162105A. Both stations are at nearly similar epicentral distance and source azimuth. Note the similar SKS amplitudes and that the amplitudes of SKKS and Sdiff are significantly different.

[6] *R* has a clear geographic pattern. Figure 3 shows *R* as a function of epicentral distance (Δ) for measurements from four subsets of data. These data sets are derived from deep (>500 km) earthquakes with moment magnitudes larger than 6.5 that exhibit SKS and SKKS signals with (>5) signal-to-noise-ratios. Groups A and B are southwest Pacific events recorded in North America and South America, respectively. Group C includes South American events recorded in Europe, and group D includes Indonesian events recorded in North America. *R* reaches an averaged peak value between $\Delta = 100^\circ$ and $\Delta = 110^\circ$ of about 0.5 and 0.3 for recordings from groups A and B, respectively. For groups A and B, the SKS core-entry points are within a broad low shear-velocity anomaly at the CMB beneath the Pacific Ocean (see Figure 1). In contrast, SKKS/SKS ratios for groups C and D can be explained by PREM synthetics. Incidentally, shear velocities near the SKS core-entry and core-exit points for the group C and D recordings are similar to those in PREM.

3. SKKS/SKS Ratios for the Pacific

[7] We analyze in more detail the data from five recent Tonga-Fiji earthquake recordings from broadband stations in the United States that make up group A. $R(\omega)$ is measured

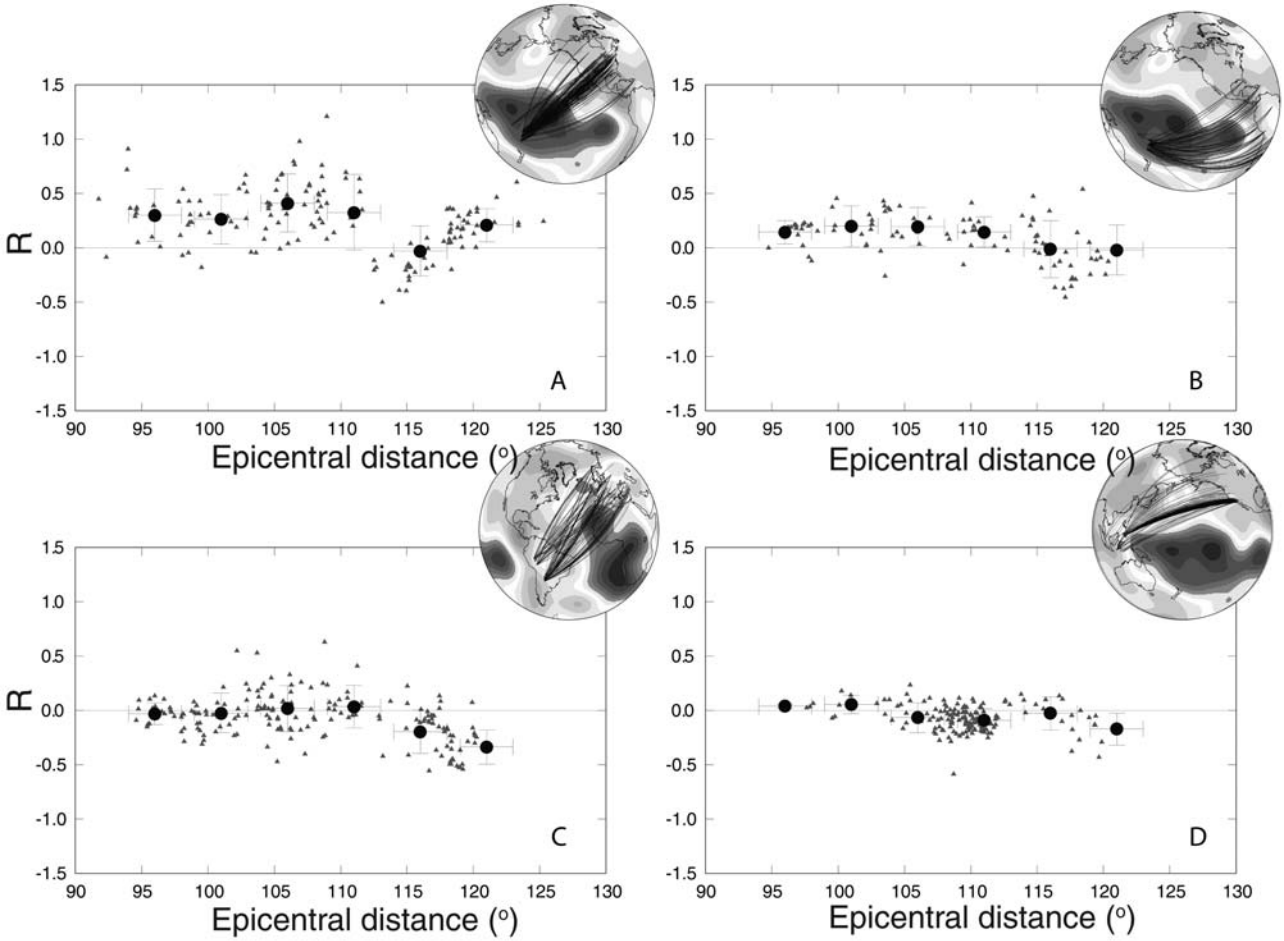

Figure 3. Measurements of *R* for data from four mantle corridors: (a) Southwest Pacific to North America, (b) Southwest Pacific to South America, (c) South America to Europe, and (d) Indonesia to North America. Open circles are individual measurements while solid circles and error bars are average values within 5° epicentral distance bins and standard deviations. Globes superposed in the upper right corner indicate the great-circle paths for each group and the shear-velocity variation at the core-mantle boundary [*Ritsema et al.*, 1999].

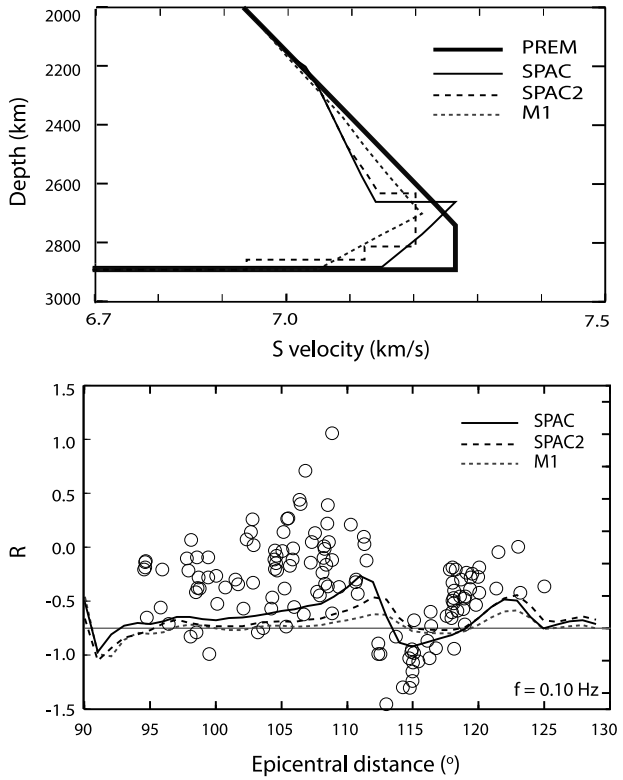

Figure 4. (top) Shear velocity profiles of models PREM, SPAC, and SPAC2, and M1. (bottom) Measurements of *R* (circles) and model predictions for model SPAC (solid line), SPAC2 (dashed line) and M1 (dotted line) at 0.10 Hz.

via spectral ratios using 1-D waveform calculations with the reflectivity method [*Fuchs and Muller*, 1971] and 3D waveform calculations for axi-symmetric structures [*Igel and Weber*, 1996; *Jahnke et al.*, 2008]. The spectral ratios can be reliably measured between periods of 5–20 s by applying spectral smoothing and multi-taper techniques. At a period of 20 s, *R* is measured beyond 98° when SKKS and SKS are well separated. Primarily due to waveform differences in the recordings and synthetics, the measurement uncertainty in *R* is about 0.05. This is an order of magnitude smaller than the variability of *R*. We apply upper mantle anisotropy corrections for those stations with available SKS splitting parameters [*Schutt and Humphreys*, 2001].

[8] We first consider three models for the Pacific lower mantle: M1 [*Ritsema et al.*, 1997], SPAC [*Russell et al.*, 2001], and SPAC2 [*Avants et al.*, 2006], which have 2–3% shear-velocity reductions in the lowermost 200–300 km of the mantle. Model SPAC includes a 10-km thick ULVZ with a P and S velocity that is, respectively, 4% and 12% smaller than in PREM.

[9] As demonstrated in Figure 4, these models with modest velocity reductions fail to reproduce the high values of *R* at 0.1 Hz (and other frequencies). Predicted values for the SKKS/SKS ratio by models M1 and SPAC2 are nearly identical to the PREM predicted values. Only SPAC reproduces the increase in *R* near 100° but underestimates its peak value.

[10] Next we consider ULVZs, embedded in the PREM velocity structure. SKKS/SKS amplitude ratios for ULVZs within more realistic models for the Pacific lower mantle (e.g., M1, SPAC, or SPAC2) produce virtually identical results. Given the considerable variability in *R* (see Figure 2), we model the ULVZ as a single layer and modify its thickness and velocity reductions from PREM. The ULVZ is present only at the core-entry region of SKS but both SKS and SKKS traverse it. At the core-exit side of SKS the seismic structure is identical to PREM.

[11] In Figure 5a, *R* is compared to predicted values for ULVZs that have thicknesses of 5, 10, and 15 km. The reductions in S and P velocity are 18% and 6%, respectively. In Figure 5b, the ULVZs are 10 km thick and have S-velocity reductions of 30%, 18%, and 6% and accompanying P-velocity reductions that are 3× smaller. In Figure 5c,

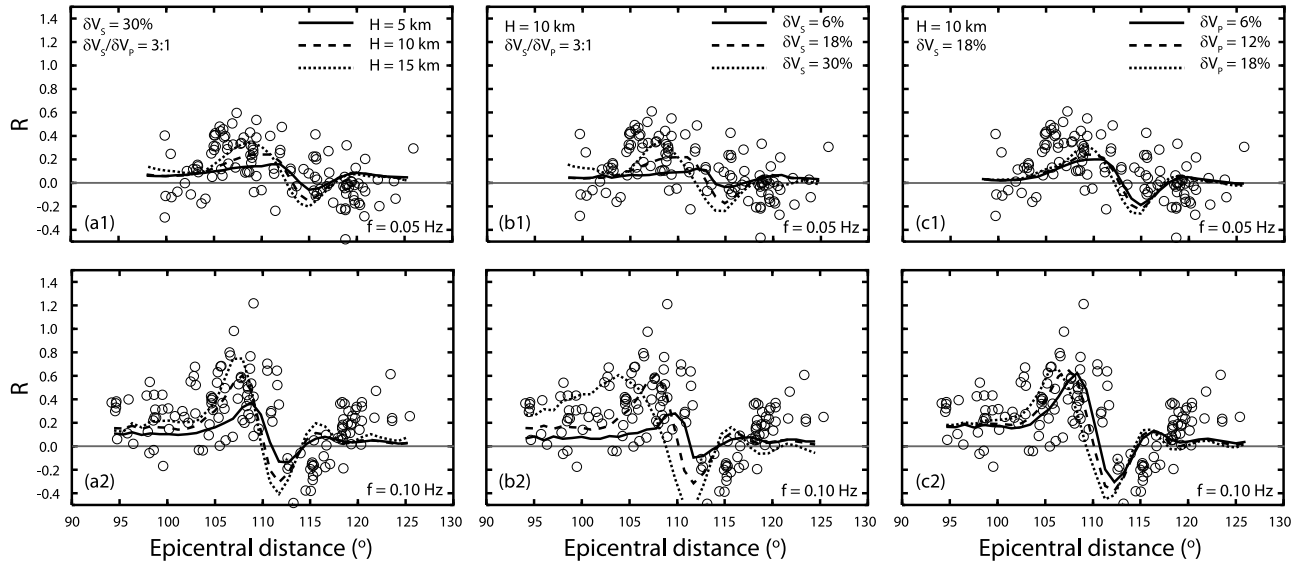

Figure 5. Measurements (circles) and model predictions (lines) of *R* at (top) 0.05 Hz and (bottom) 0.1 Hz for ULVZs at the SKS and SKKS core-entry points. Varied are (a) ULVZ thickness, (b) V_S reduction, and (c) the ratio of the V_S and V_P reductions.

we consider ULVZs with a thickness of 10 km, a S-velocity reduction of 18%, and P-velocity reductions of 6%, 12%, and 18%. Thus the ratios of S and P velocity reductions are 3:1, 3:2, and 3:3, which are expected when melts are present (3:1) [e.g., *Williams and Garnero*, 1996; *Revenaugh and Meyer*, 1997], or when the ULVZ is compositionally distinct (3:3).

[12] We analyze the match to R at frequencies of $f = 0.1$ Hz and $f = 0.05$ Hz, the upper and lower frequency limits for which R is measured most reliably. R is consistently larger than 0 for distances up to 108°. R is negative between 108° and 115° due to the formation of SP_dKS for PREM. The oscillation in R is strongest at 0.1 Hz. Observed R values reach around 0.2 at a distance longer than 120°, which cannot be reproduced accurately by our ULVZ models.

[13] R is highest for the thickest ULVZs with the largest velocity reductions and R's maximum value shifts to the shortest distances. These trends are due to the advanced move-out of SP_dKS from SKS and the reduction of the SKS amplitude. For the ULVZ structures examined in Figure 5, the maximum values of R are larger for $f = 0.1$ Hz and R peaks approximately 5° earlier. The frequency dependence of R can, in principle, help reduce the modeling trade-off between thickness and velocity.

[14] As pointed out previously [e.g., *Garnero and Helmberger*, 1998], there is a trade-off between thickness and shear velocity reduction. For thickness between 5–15 km, when the high-frequency SKS waveforms are matched best [*Stutzmann et al.*, 2000], we resolve a shear-velocity reduction of 18%∼30%. Values that are comparable to those inferred from SP_dKS traveltime studies [e.g., *Thorne and Garnero*, 2004]. Especially at $f = 0.1$ Hz, the high R values for distances smaller than 108° are reproduced best for a ratio of S and P-velocity reductions of 3:2.

4. Discussion and Conclusions

[15] The scatter in R is large and not due to measurement error. Figure 2 demonstrates that SKS and SKKS (and Sdiff) amplitudes from nearly co-located (from a teleseismic point of view) stations can differ significantly. Sources for this scatter may include anisotropy at the base of the mantle [*Fouch et al.*, 2001; *Long*, 2009], shear velocity gradients [*To et al.*, 2005], and core mantle boundary topography [*Restivo and Helffrich*, 2006]. The scatter indicates the presence of fine-scale structure that cannot be addressed with our simplified models and synthetics.

[16] We emphasize therefore the overall trends in the SKKS/SKS amplitude ratios. First, SKKS/SKS amplitude ratios are anomalous with respect to standard model predictions only when SKS core-entry points are within the low shear-velocity region beneath the Pacific. Second, Tonga-Fiji earthquake recordings from North America show a systematic variation with epicentral distance (95°–125°) and signal frequency. This cannot be explained by 1D shear-velocity profiles that include 2–3% shear-velocity reductions in the lowermost several hundreds of kilometers of the mantle. Rather, our long-period data require the presence of thin (∼10–20 km) Ultra-Low Velocity Zones (ULVZ) in which the shear velocity is reduced by 20–30%, corroborating previous (short period and broadband) modeling efforts.

[17] **Acknowledgments.** Data have been provided by GEOSCOPE and IRIS. All Figures were produced using the GMT software [*Wessel and Smith*, 1995]. We thank Edward Garnero and Matt Fouch for software anisotropy data. We thank two anonymous reviewers for useful suggestions. The research has been funded by NSF grant EAR-0609763.

References

Avants, M., T. Lay, S. A. Russell, and E. J. Garnero (2006), Shear velocity variation within the D″ region beneath the central Pacific, *J. Geophys. Res.*, *111*, B05305, doi:10.1029/2004JB003270.

Choy, G. (1977), Theoretical seismograms of core phase calculated by frequency-dependent full-wave theory, and their interpretation, *Geophys. J. R. Astron. Soc.*, *5*(2), 275–311.

Dziewonski, A. M., and D. L. Anderson (1981), Preliminary reference Earth model, *Phys. Earth Planet. Inter.*, *25*, 297–356.

Fouch, M., K. Fischer, and M. Wysession (2001), Lowermost mantle anisotropy beneath the Pacific: Imaging the source of the Hawaiian plume, *Earth Planet. Sci. Lett*, *190*(3–4), 167–180.

Fuchs, K., and G. Muller (1971), Computation of synthetic seismograms with the reflectivity method and comparison with observations, *Geophys. J. R. Astron. Soc.*, *23*(4), 417–433.

Garnero, E., and D. Helmberger (1996), Seismic detection of a thin laterally varying boundary layer at the base of the mantle beneath the central-Pacific, *Geophys. Res. Lett.*, *23*(9), 977–980.

Garnero, E., and D. Helmberger (1998), Further structural constraints and uncertainties of a thin laterally varying ultralow-velocity layer at the base of the mantle, *J. Geophys. Res*, *103*(B6), 12,495–12,509.

Garnero, E., J. Revenaugh, Q. Williams, T. Lay, and L. Kellogg (1998), Ultralow velocity zone at the core-mantle boundary, in *Core-Mantle Boundary Region*, *Geodyn. Ser.*, vol. 28, pp. 319–334, AGU, Washington, D. C.

Hernlund, J. W., and P. J. Tackley (2007), Some dynamical consequences of partial melting in Earth's deep mantle, *Phys. Earth Planet. Inter.*, *162*(1–2), 149–163.

Hutko, A. R., T. Lay, and J. Revenaugh (2009), Localized double-array stacking analysis of PcP: D″ and ULVZ structure beneath the Cocos plate, Mexico, central Pacific, and north Pacific, *Phys. Earth Planet. Inter.*, *173*(1–2), 60–74.

Idehara, K., A. Yamada, and D. Zhao (2007), Seismological constraints on the ultralow velocity zones in the lowermost mantle from core-reflected waves, *Phys. Earth Planet. Inter.*, *165*(1–2), 25–46.

Igel, H., and M. Weber (1996), P-SV wave propagation in the Earth's mantle using finite differences: Application to heterogeneous lowermost mantle structure, *Geophys. Res. Lett.*, *23*(5), 415–418.

Jahnke, G., M. S. Thorne, A. Cochard, and H. Igel (2008), Global SH-wave propagation using a parallel axisymmetric spherical finite-difference scheme: Application to whole mantle scattering, *Geophys. J. Int.*, *173*(3), 815–826.

Long, M. (2009), Complex anisotropy in D″ beneath the eastern Pacific from SKS-SKKS splitting discrepancies, *Earth Planet. Sci. Lett.*, *283*, 181–189.

Ni, S., and D. V. Helmberger (2003), Ridge-like lower mantle structure beneath South Africa, *J. Geophys. Res.*, *108*(B2), 2094, doi:10.1029/2001JB001545.

Restivo, A., and G. Helffrich (2006), Core-mantle boundary structure investigated using SKS and SKKS polarization anomalies, *Geophys. J. Int.*, *165*(1), 288–302.

Revenaugh, J., and R. Meyer (1997), Seismic evidence of partial melt within a possibly ubiquitous low-velocity layer at the base of the mantle, *Science*, *277*, 670–673.

Ritsema, J., E. Garnero, and T. Lay (1997), A strongly negative shear velocity gradient and lateral variability in the lowermost mantle beneath the Pacific, *J. Geophys. Res.*, *102*(B9), 20,395–20,411.

Ritsema, J., H. J. van Heijst, and J. H. Woodhouse (1999), Complex shear velocity structure imaged beneath Africa and Iceland, *Science*, *286*, 1925–1928.

Rondenay, S., and K. M. Fischer (2003), Constraints on localized core-mantle boundary structure from multichannel, broadband SKS coda analysis, *J. Geophys. Res.*, *108*(B11), 2537, doi:10.1029/2003JB002518.

Rost, S., and E. J. Garnero (2006), Detection of an ultralow velocity zone at the core-mantle boundary using diffracted PKKPab waves, *J. Geophys. Res.*, *111*, B07309, doi:10.1029/2005JB003850.

Rost, S., and J. Revenaugh (2001), Seismic detection of rigid zones at the top of the core, *Science*, *294*, 1911–1914.

Rost, S., and J. Revenaugh (2003), Small-scale ultralow-velocity zone structure imaged by ScP, *J. Geophys. Res.*, *108*(B1), 2056, doi:10.1029/2001JB001627.

Russell, S., C. Reasoner, T. Lay, and J. Revenaugh (2001), Coexisting shear- and compressional-wave seismic velocity discontinuities beneath the central Pacific, *Geophys. Res. Lett.*, *28*(11), 2281–2284.

Schutt, D., and E. Humphreys (2001), Evidence for a deep asthenosphere beneath North America from western united states SKS splits, *Geology*, *29*(4), 291–294.

Silver, P., and C. Bina (1993), An anomaly in the amplitude ratio of SKKS SKS in the range 100–108° from portable teleseismic data, *Geophys. Res. Lett.*, *20*(12), 1135–1138.

Simmons, N. A., and S. P. Grand (2002), Partial melting in the deepest mantle, *Geophys. Res. Lett.*, *29*(11), 1552, doi:10.1029/2001GL013716.

Souriau, A., and G. Poupinet (1991), A study of the outermost liquid core using differential travel-times of the SKS-phase, SKKS-phase and S3KS-phase, *Phys. Earth Planet. Inter.*, *68*(1–2), 183–199.

Stutzmann, E., L. Vinnik, A. Ferreira, and S. Singh (2000), Constraint on the S-wave velocity at the base of the mantle, *Geophys. Res. Lett.*, *27*(11), 1571–1574.

Thorne, M. S., and E. J. Garnero (2004), Inferences on ultralow-velocity zone structure from a global analysis of SPdKS waves, *J. Geophys. Res.*, *109*, B08301, doi:10.1029/2004JB003010.

To, A., B. Romanowicz, Y. Capdeville, and N. Takeuchi (2005), 3D effects of sharp boundaries at the borders of the African and Pacific superplumes: Observation and modeling, *Earth Planet. Sci. Lett.*, *233*(1–2), 137–153.

Wessel, P., and W. H. F. Smith (1995), New version of the Generic Mapping Tools released, *Eos Trans. AGU*, *76*, 329.

Williams, Q., and E. Garnero (1996), Seismic evidence for partial melt at the base of Earth's mantle, *Science*, *273*, 1528–1530.

J. Ritsema and Y. Zhang, Department of Geological Sciences, University of Michigan, 1100 North University Avenue, Ann Arbor, MI 48109, USA. (yzhan@umich.edu)

M. S. Thorne, Department of Geology and Geophysics, University of Utah, 135 South 1460 East, Salt Lake City, UT 84112, USA.